Keränen Lauri Veikko Samuli

Nano- and femtosecond laser coloring methods and their investigation using Scanning Electron Microscopy and X-ray Photoelectron Spectroscopy

Bachelors' degree

Faculty of science

Physics

20.11.2019

Contents

1 Introduction

The research of surfaces of materials has been a popular subject in the 20th and 21st century. Methods and equipment used in analyzing the structure and the composition of the first few atomic layers at the surface have improved since then. This opens the possibility to obtain information of naturally occurring phenomena along with their application in research and industry. One of these methods include laser induced color. Color produced by beaming the surface with a laser can be achieved on the surface of steel among with cadmium, copper and titanium and other transition metals as the electronic structure is favorable for creating metal oxides which produce their intrinsic color. Further, laser treatment is the ecological alternative for environmentally consuming coloring methods, such as painting and printing. In the future it will provide a way to produce a low cost, highly corrosion resistant colors.

Surface studies are an important field in the modern world as they improve the overall efficiency of the device, for example surface of solar panels can be given water and corrosion resistant properties. To visualize the changes in the surface micro-structure post laser coloration, scanning electron microscopy (SEM) probe has been utilized. Regarding markings and light interference, same kind of structure is found on, for example, butterfly wings. Microstructure and light interference are a lifelong quality if the surface structure, unless it is broken or destructed in any way.

X-ray photoelectron spectroscopy (XPS) is a surface sensitive method for analyzing the surface of materials with a large variety ranging from metals to biomaterials. It gives information about the elemental composition and chemical state of the elements on the sample surface. XPS contributes as one of the important methods in analyzing the properties of nanomaterials as it offers to determine the oxidation states of the atoms along with the chemical environment of the surface species.

This thesis summarizes the laser induced coloring methods through a nano- and femtosecond laser induced structures on steel surfaces and their investigation using SEM and XPS. Firstly, the basics of atom physics and the understanding of interaction of matter with radiation through photoemission, Auger emission and x-ray production are introduced. The theory of XPS is also discussed briefly. Further, the potential and applications of surface studies are covered using XPS. Followed by the introduction to XPS, we discuss two steel 304 samples chosen for the

current laser treatment, one with a nanosecond laser and the other with a femtosecond laser. During the laser treatment, a periodic surface structure was formed on both surfaces. But because the laser treatment was done with different pulse frequencies on different samples, the color on the surfaces came from different sources. It either came from the intrinsic color of steel oxides and spinel formed, or the light interfering with the surface treated with the laser. From these samples a spectrum was measured with the X-ray photoelectron spectroscope that was analyzed to determine the components on the steel surfaces.

2 Research methodology: tools and techniques

In the brink of the 20th century when W. K. Röntgen discovered X-rays, the source of these rays was unclear among with the correct structure of an atom. The development of the atomic model lead to the understanding of X-rays. In 1897 in his Nobel Prize winning discovery J. J. Thomson discovered electrons in an atom by assuming so called "cathode rays", a stream of negatively charged electrons the path of which could be bent by an electromagnetic field. Later he gave plum pudding model of an atom. This model was found to be inaccurate by Ernest Rutherford in his famous experiment where he fired positively charged alpha particles at a gold foil. According to Thomson model the particles were supposed to pass through the atom but some reflected in opposite directions which in 1911 lead to Rutherford's model of a concentrated positive charge in the middle of an atom and electrons orbiting around the positive charge. The problem with this was that particles in accelerating motion are supposed to emit electromagnetic radiation and thus emit energy and in conclusion the electrons would collapse into the nucleus and the atom would disintegrate, which is not the case. In 1913 Niels Bohr suggested stable electron orbits where electrons on their defined orbits would not lose energy while in accelerating motion. This was nearly the right answer to the atomic model but was later in 1926 refined by E. Schrödinger when he applied Heisenberg uncertainty principle to the model of an atom and suggested that electrons do not move in set orbits, but are impossible to locate exactly in a cloud of probability around the nucleus, different electrons have different energies inside the atom which come from them having different quantum states.[1]

2.1 Radiation, particle emission and XPS physics

When an electron is emitted form an inner shell of an atom, an electron from an outer shell takes its place and as the atom moves from a higher to a lower energy state, a photon is emitted with an energy equivalent to the difference of the binding energies of these states. The frequency of an electron (ν) is the energy difference divided by Planck's constant, and if the energy (frequency) of the emitted photon is high enough, the emitted radiation belongs to the X-ray region in the electromagnetic spectrum and is given by[2]

$$\nu = \frac{E_{n1} - E_{n2}}{h} .$$

Where the wavelength of X-rays is in the range of soft X-rays ($10nm - 100pm$) to hard X-rays ($100pm - 10pm$).

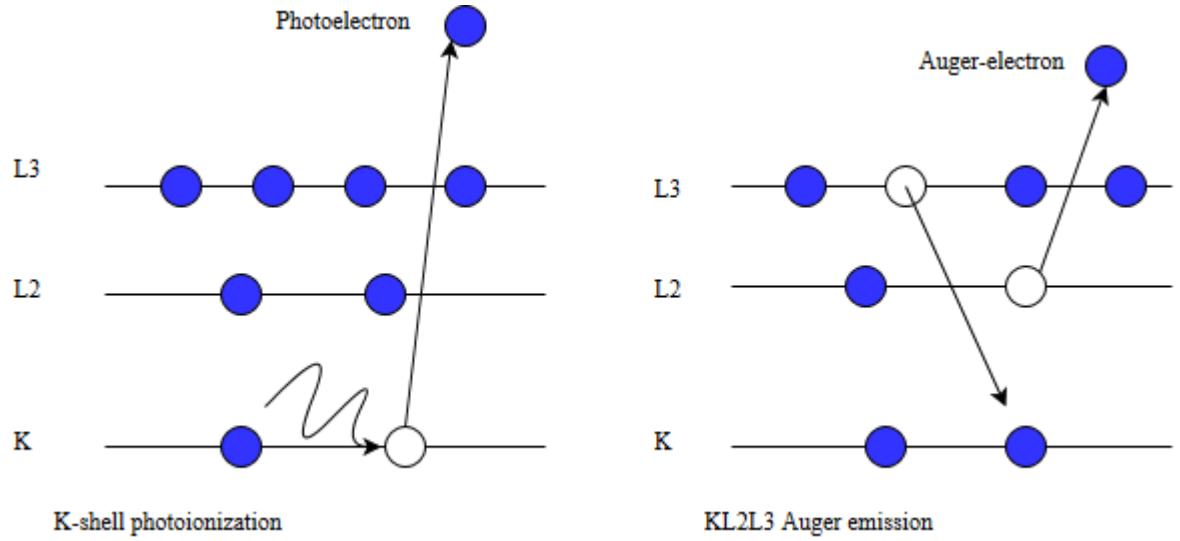

Fig. 1. Photoelectron and Auger electron emission processes

There is also a possibility of an emission of an Auger electron in the process instead, when the free energy from the emission goes to another electron which is then emitted. X-rays can be emitted in multiple ways such as, an atom emitting or absorbing an electron from an inner shell or when a charged particle is in accelerating motion and particles' energy spectrum is continuous. The vacancy in the shell of an atom can be realized by bombarding the atom with photons or particles such as neutrons or electrons. In the case of particles, the kinetic energy of a particle must be much greater than the ionization energy and only a fraction goes to ionizing the atom. In case of the photon the whole photon is absorbed by the atom and the kinetic energy of the electron emitted can be calculated from the energy of the photon and the ionization energy of the electron. X-rays can be emitted in radioactive decay or by electron capture when an electron from the K-shell is absorbed into the nucleus and the vacancy in the inner shell is filled by an electron from an outer shell. X-rays can also form by using thermal energy when a heated object radiates on a wavelength of $\lambda = \frac{hc}{kT}$, or by synchrotron radiation where the particles with a velocity near the speed of light in a vacuum in circular motion change direction and are in an

accelerating motion they emit radiation. Based on the same phenomenon of accelerating particles emitting radiation the method popularly used in X-ray photoelectron spectroscopy to generate the X-rays is bremsstrahlung or "braking radiation". In bremsstrahlung a metallic anode is bombarded by high-energy electrons, and because metals have generally large atomic numbers the acceleration of electrons is high and the whole kinetic energy goes into radiation if the electron is completely stopped.

2.2 Laser coloring methods

The potential of nanomaterials lies in the interest towards circuit elements, optical and photonic devices, biotechnical applications, and the possibilities to construct new materials with these structures. For electronic elements, there is a possibility to produce surfaces with enhanced conducting properties by varying the electron structure and the amount of free valence electrons. Optical traits and light reflective qualities can be produced. (e.g. the laser induced color) And for example biotechnical applications, there is an essential role for nanomaterials in making implants and making them durable. Effective methods in making nanomaterials in the modern world have been proven to improve the qualities of many products, many of these properties have been taken an example from nature; leaves have self-cleaning properties, butterflies, snakes and peacocks have structural color to mention a few.

The methods and technologies used to analyze the material to see what kind of structures need to be produced and producing these shapes artificially have improved along with the knowledge of the properties of the surface. The chemical coloration methods of metals for decorative purposes have been time and most importantly environmentally consuming methods even in the 21st century, though widely popular because of the beautiful spectrum of possible colors, excellent performance and resistance against corrosion. Therefore, the laser coloring method gives an outstanding alternative for the purpose of coloration. Such color has been successfully produced with a femtosecond laser and structural color, but the method is high cost because of the price of femtosecond lasers, and it is not suitable for industrial productions. The alternative nanosecond laser method was believed to be able to produce only a limited range of colors by tuning the laser parameters. But as the range of possible colors has been extended over time, the method in which the colors are produced remains unclear. There is little to none color from light interference, as the structure of the surface on the nanoscale is still much larger compared to the wavelength of visible light.[3] Fig.2 shows a simplified instrumentation for laser coloring,

the beam is directed with mirrors and then focused with a lens to the sample that is set up on a platform that moves in all directions.

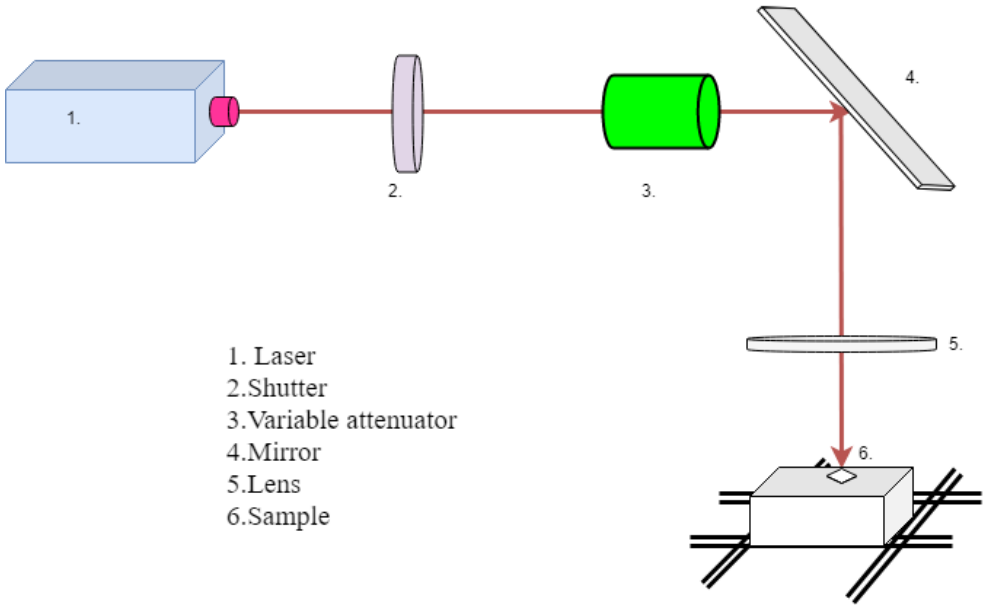

Fig. 2. Instrumental setup for laser coloring

Three different sources are used for color producing in laser treatment. The first source is the color from the thin oxide film and the intrinsic colors of the oxides on the surface, or when the light is reflected from the film and the surface of the metal simultaneously, and when the length of the route that the light travels through the film is the multiple of the wavelength of the specific color, then the color is enhanced. The second source is the color from the interference of the light with the nanostructure caused with femtosecond- or picosecond lasers on the surface. This color can be observed only from specific angles with respect to the surface. And third one is, from the structural colors and surface plasmon resonance.[4]

2.3 XPS as a characterization tool

X-ray photoelectron spectroscopy is a surface sensitive method for analyzing the surfaces of materials with a large variety ranging from metals to biomaterials. It gives information about the elemental composition, chemical state of the elements on the sample surface, which contributes to it being one of the important methods in analyzing the properties of nanomaterials as it is also possible to determine the oxidation states of the atoms along with the chemical

environment of the surface species. XPS uses soft X-rays with wavelength in the range of 10nm-100 pm. When a surface is irradiated with this kind of radiation, the electrons in the materials surface atoms are emitted from the surface because of photoelectric effect. The photoelectric effect happens when electromagnetic waves that are intensive enough are pointed at a surface. When the energy of the photon is greater than the binding energy of the electron, the electron is emitted from the surface. The kinetic energy spectrum of the emitted electrons can be measured, and so can be used to determine the composition at the surface. Relation between kinetic energy of emitted electron and energy of X-ray is given by,

$$E_b = h\nu - E_k - \Phi$$

where E_b is the binding energy of the electron, h is Planck's constant ν is the frequency of the X-rays, E_k is the kinetic energy of the photoelectron and Φ is the work function dependent on the spectrometer, $h\nu$ is known and the kinetic energy of the photon can be determined experimentally.[5]

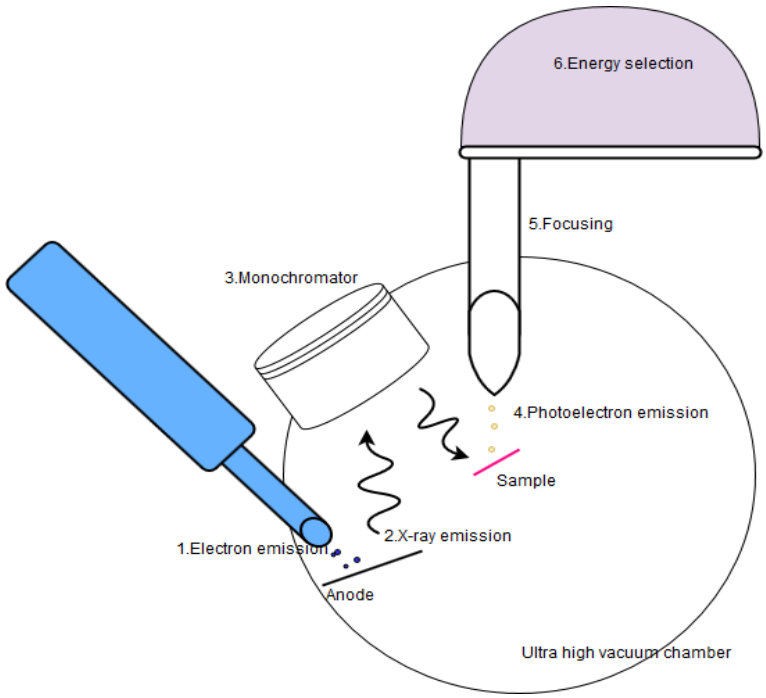

Fig. 3. Instrumental setup of X-ray photoelectron spectroscope.

The XPS spectrum is the plot of number of emitted electrons per energy interval versus their binding/kinetic energy. The binding energies form a continuous spectrum of various peaks appearing from different atoms as they have different binding energies. In the spectrum, a doublet can be observed because of different spin states. The observed peaks in doublets are from spin orbit splitting where two possible states have different binding energies because of the spin angular momentum number $s = \pm\frac{1}{2}$ has two possible states, spin up and spin down, so the sum of s and angular momentum quantum number l, $j = l + s$ gives on subshell p the values $j = \frac{1}{2}\ and\ \frac{3}{2}$. The area ratio of the two peaks depends on what subshell the spin component comes from, excluding the s level where $l = 0$ and no doublet can be observed.

Table.1. Different quantum number values and area ratios.

Subshell	j values	Area ratio
p	1/2, 3/2	1:2
d	3/2, 5/2	2:3
f	5/2, 7/2	3:4

The XPS spectra of different elements vary. For example, different oxides on metal surfaces have different binding energies as well as the different chemical states. Some of the peaks come from plasmon loss which is the result of interaction of the photoelectron and the other electrons on the material. The X-rays can also emit electrons from atoms deeper than the few nanometers into the surface, while escaping, these electrons can collide with the other atoms and their kinetic energy is affected which shows up on the XPS spectra as the background of the spectrum.[6]

2.4 SEM

SEM is used to analyze the surface morphology of a material. SEM is a reflection-based technique where the electrons are produced from the tungsten filament by thermionic emission. The emitted electrons are accelerated by an electric field and the beam is condensed with electromagnetic lenses. Various possible interactions of the electron beam with the surface are: backscattering, X-rays, Auger electrons and secondary electrons that have low energy. These can be detected and used for imaging. The X-rays formed during the process can be used for

obtaining information about the elements present in the region. The resolution of the device depends on the beam size and the accelerating voltage.

3 Results

Stainless steel substrates employed in the work are mechanically polished AISI 304 and 301 LN slabs for nanosecond and femtosecond laser treatments respectively. The nominal compositions of these alloys are ~ Fe-18.0Cr-2.0Mn-8.0Ni-1.0Si and Fe-16.5Cr-2.0Mn-6.0Ni-1.0Si (wt%). Different lase parameters such as scanning speed, repetition rate and pulse width were used for nanosecond laser to produce three different colors: yellow, red and blue. Thermo Fisher Scientific ESCALAB 250Xi XPS System, with an energy resolution of $< 0.45eV$ using $Al - K$ anode as the X-ray source was used. The following figures 5.-11. show the peak fittings made with Thermo Scientific Avantage software, each peak count/s errors varied on a range from $100 - 300\frac{C}{s}$ as taken from the Avantage software Nonlinear least squares window view. The error for the peak positions is likely to be large (1-1.5eV) as for example in the manganese fit the different oxides are combined in one single peak, and other transition metal species have energy structures that overlap in a way it makes it difficult to analyze, however the error should vary from $0.1 - 0.2eV$.

3.1 Laser treatment results

The possibility of the structural color was taken into consideration and studied by taking SEM (scanning electron microscope) images of the femtosecond laser treated surface and all the different colors from the nanosecond laser treated surfaces. The figures 4. a-c show the microscale structure of the surfaces. In nanosecond markings some randomly oriented wrinkles can be seen in microscale, the only periodic structure can be imagined on the red colour, in image 4.(c), where the scale is still around $7 - 12\mu m$, which makes it hard for interference to be the source of the coloration. In the image 4.d) clear grooves are seen $2 - 6\mu m$ apart horizontally and in much smaller scale vertically.

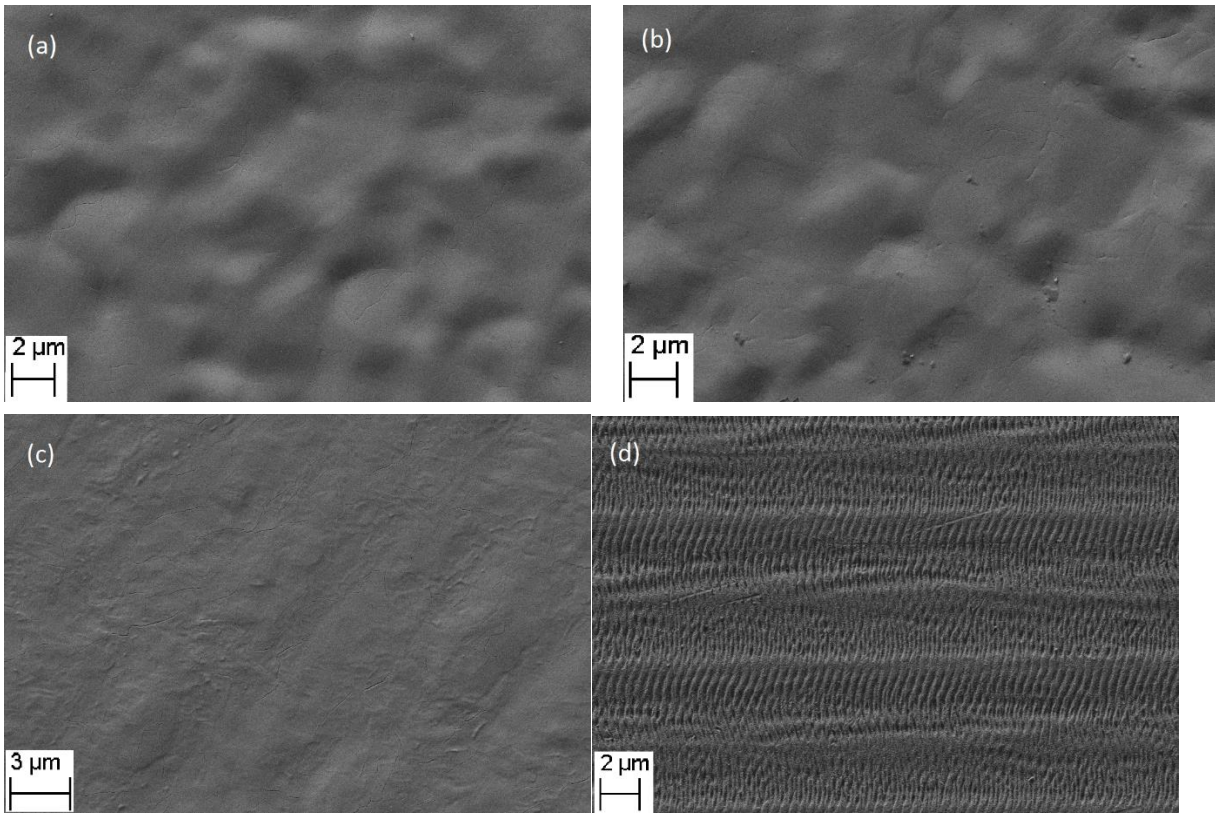

Fig. 4. SEM images of the laser treated surfaces, (a),(b) and (c) are nanosecond laser treated with colors as (a)yellow (b)blue (c)red and (d) corresponds to the femtosecond treated surface

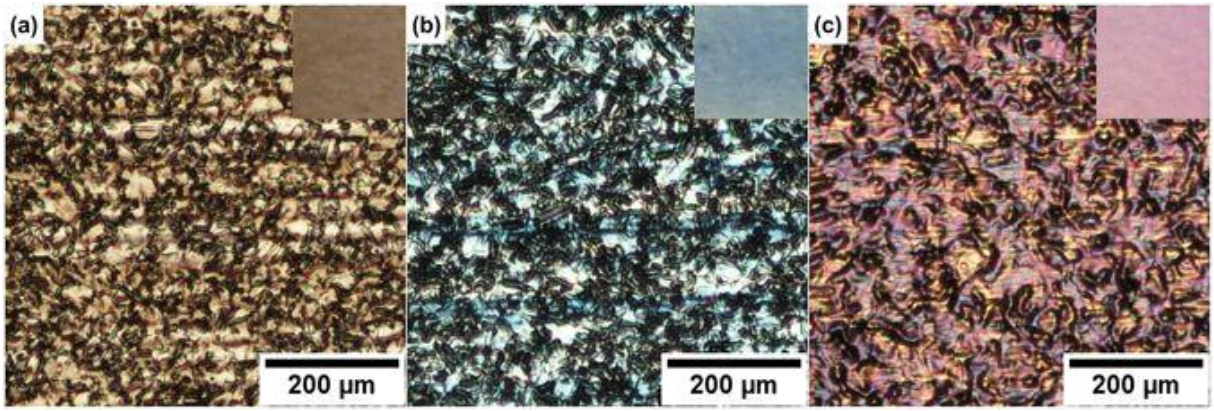

Fig. 5. The nanosecond laser treated steel. XPS and SEM are measured from three different color spots.

3.2 XPS scan fittings

XPS measurements were taken from all the different colors of the nanosecond and the femto-second markings. The differences between nanosecond laser induced surface composition and the femtosecond laser induced surface composition can be seen from the difference in peak position in the iron scan along with the presence of nickel in femtosecond scans (Tables 2.-5., fig 12.). Nanosecond yellow, red and blue refer to the colors seen on the image of Figure 5.

Table. 1. The elemental composition of the yellow surface via binding energy position, FWHM and areas of the peak.

Name	***Peak BE***	***FWHM eV***	***Area (P) CPS.eV***	***Atomic %***	***Q***
Cr_2O_3	575.79	1.13	3965.86	15.78	1
Cr spinel	576.91	1.41	5708.29	22.73	1
Cr_2O_3 sat	578.25	1.68	2751.54	10.96	1
Cr spinel sat	580.46	2.40	963.96	3.84	1
Fe spinel	709.26	1.78	30718.42	13.14	1
Fe_2O_3	710.40	1.42	18905.82	8.09	1
Fe oxide sat.	711.49	1.60	23381.87	10.01	1
FeO	708.12	1.33	8265.90	3.53	1
MnO	639.98	1.32	9101.45	4.58	1
Mn spinel	641.70	1.19	4684.63	2.36	1
Mn_2O_3	640.97	1.19	5613.30	2.83	1
Mn_2O_3 sat.	642.47	1.06	2924.54	1.47	1
Oxide sat.	643.26	0.96	1328.33	0.67	1

For the nanosecond markings, the composition is mostly from chromium, iron, manganese and nickel, the elements with a smaller value have been left out as the impact is insignificant compared to the dominant ones. In Fig 5. the Fe scans have been compared. It consists of two peaks with one being from $Fe2p_{1/2}$ and the other from $Fe2p_{3/2}$ of which the latter has been

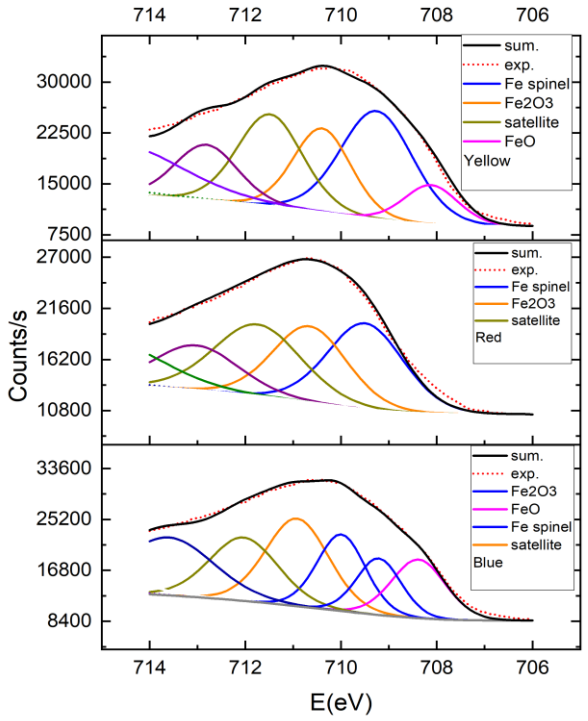

Fig. 6. Fitted XPS spectra for iron corresponding to yellow, red and blue colored surfaces

included in the image. Similar components can be found on each of the scans. The peak around $708.38eV$ can be identified as FeO oxide of iron, and the second peak at $709.21eV$ as the spinel compound formed while the laser treatment. After the main components there can be found peaks that correspond as the satellites for the spinel and the oxide. On the Fig 6. chromium scan, the main peaks can be divided into three doublet peaks identified as Cr_2O_3 at $575.73eV$ $Cr-spinel$ at $576.77eV$. Respective satellites can be found in between similarly to the Fe scan. The manganese oxide peaks are fitted the best way possible, there can be separated the manganese spinel compound at $639.76eV$, the manganese oxides peaks from $640.5eV$ to $642eV$.[9] These peaks all have satellite peaks around the satellites from $Mn2O3$ and the spinel satellites which may have an effect on the width of the spinel satellite and so to the atomic percentage, which is larger than expected. The $Ni2p$ scan has not been included as the atomic percentage of nickel on the surface has dropped to near zero from the amount in commercial 304 steel which has 8-10% nickel in it. In an earlier study there was an analysis of the different components' contribution to the color, for example chromium was noted to be the main reason for red color, and iron to be the cause of blueish tones of the color ranging from "grey-blue, violet blue to even dark green".[7,8,9]

Table. 2. The elemental composition of the blue surface via binding energy position, FWHM and area of the peak.

Name	Peak BE	FWHM eV	Area (P) CPS.eV	Atomic %	Q
Cr2O3	575.79	1.13	3965.86	9.63	1
Cr spinel	576.91	1.41	5708.29	13.87	1
Cr2O3 sat	578.25	1.68	2751.54	6.69	1
Cr spinel sat	580.46	2.40	963.96	2.35	1
Mn spinel	639.99	1.59	12087.31	30.29	1
Mn2pO3	641.05	2.10	10715.36	2.17	1
Mn spinel sat	642.20	1.58	5283.95	13.26	1
Mn2pO3 sat	643.60	1.44	2629.95	0.53	1
Fe spinel	709.26	1.78	30718.42	8.02	1
Fe2O3	710.40	1.42	18905.82	4.94	1
Fe oxide sat	711.49	1.60	23381.87	6.11	1
FeO	708.12	1.33	8265.90	2.16	1

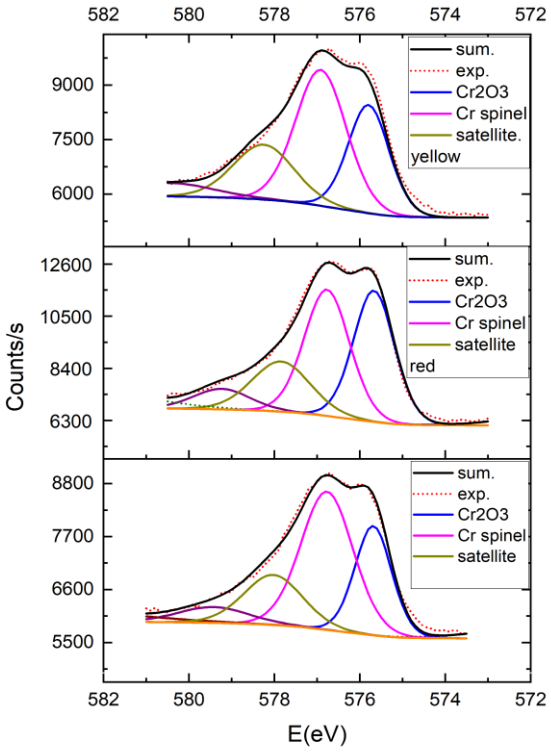

Fig. 7. Fitted XPS spectra for chromium corresponding to yellow, red and blue surfaces

The blue color from the nanosecond laser treatment shows similarities to the yellow color as the FeO found from $708.12eV$ and the spinel at $709.26eV$ correspond the peaks from the yellow color spectrum. The small discrepancies with the positions on the spectrum in majority come from the fitting of the data, as it is not 100% accurate, or in a smaller scale the fluctuations in measurements between the two samples. On the chromium scan in Fig 6. the Cr_2O_3 at $575.79eV$, $Cr-spinel$ at $576.91eV$. The manganese spinel was found at $639.99eV$ and the manganese oxides from $641.05eV$ to $642.5eV$ seen in Fig 17. (MnO, Mn_2O_3).[7 8 9]

Table. 3. The elemental composition of the red surface via binding energy position, FWHM and areas of the peak.

Name	*Peak BE*	*FWHM eV*	*Area (P) CPS.eV*	*Atomic %*	*Q*
Cr_2O_3	575.69	1.13	6424.73	22.80	1
Cr spinel	576.77	1.25	6900.12	24.50	1
Cr spinel sat	579.37	1.56	1517.61	5.39	1
Cr_2O_3 sat	577.84	1.60	3512.10	12.48	1
Fe spinel	709.50	1.87	18408.02	7.02	1
Fe_2O_3	710.66	1.83	15896.58	6.07	1
Fe oxide sat.	711.75	1.84	17540.28	6.70	1
MnO	639.90	1.19	9728.91	4.36	1
Mn_2O_3	640.73	1.37	7748.70	3.48	1
Mn spinel	641.33	1.35	6689.08	3.00	1
Mn_2O_3 sat	641.94	1.27	4659.40	2.09	1
Mn oxide sat	642.78	1.56	4689.49	2.11	1

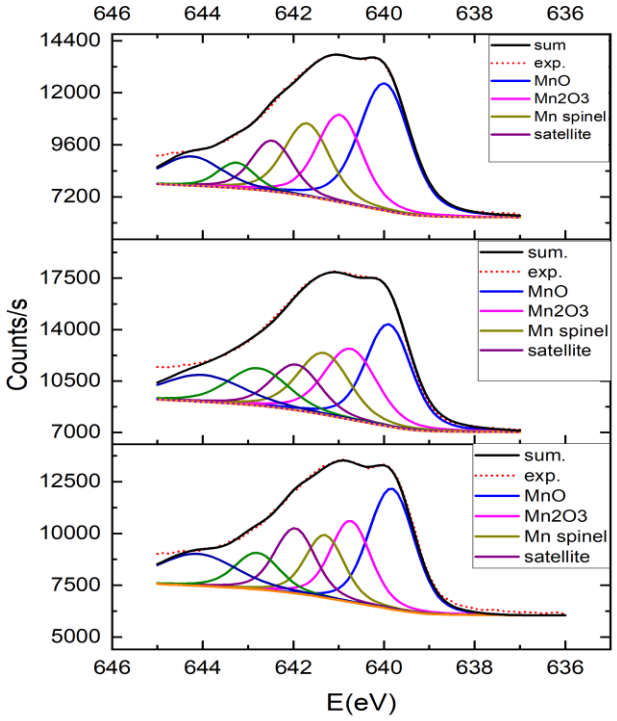

Fig. 8. Fitted XPS spectra for manganese corresponding to yellow, red and blue colored surfaces

The red color correlates the last two in the compounds found on the surface. In the iron scan in Fig5., the iron oxide at $710.66eV$ spinel at $709.50eV$. In the chromium scan in Fig 6. chromium oxide at $575.69eV$ $Cr-spinel$ at $576.77eV$. The manganese oxides around the $642eV$ mark and the spinel compound at $639.93eV$ seen in Fig 7. The amount of nickel stays low in all the samples. As a result, from the treatment in the nanosecond case the nickel is left under the spinel and oxide compounds' thin film to the bulk of the material.[10] The differences of the three nanosecond samples appear in the atomic percentages of the

compounds. This can be affiliated to the coloration methods and the fact that different elements contribute different colors, and as the laser parameters are changed though the pulse frequency stays the same, the conditions in the surface change in some amount. The changes are not too drastic as there are notable similarities in the spectra, but even a small change in the number of elements contributes in the change in color. [7 8 9]

Table. 5. The elemental composition of the femtosecond laser treated surface via binding energy position, FWHM and areas of the peak.

Name	***Peak BE***	***FWHM eV***	***Area (P) CPS.eV***	***Atomic %***	***Q***
Ni metal	852.76	1.15	5315.13	35.94	1
Ni metal sat	859.06	2.55	829.56	5.64	1
NiO	855.18	2.35	1175.19	7.96	1
Fe metal	706.53	1.05	23147.41	14.21	1
FeO	708.38	1.02	10196.82	6.26	1
Fe_2O_3	709.47	1.57	20854.66	12.82	1
Cr metal	573.99	1.25	2929.46	2.18	1
Cr(III) oxide	575.76	1.17	6854.92	5.11	1
Cr(III) sat.	576.75	1.43	11292.04	8.43	1
Mn_2O_3	640.24	1.26	1690.07	1.22	1
Mn metal	638.60	1.38	298.28	0.22	1

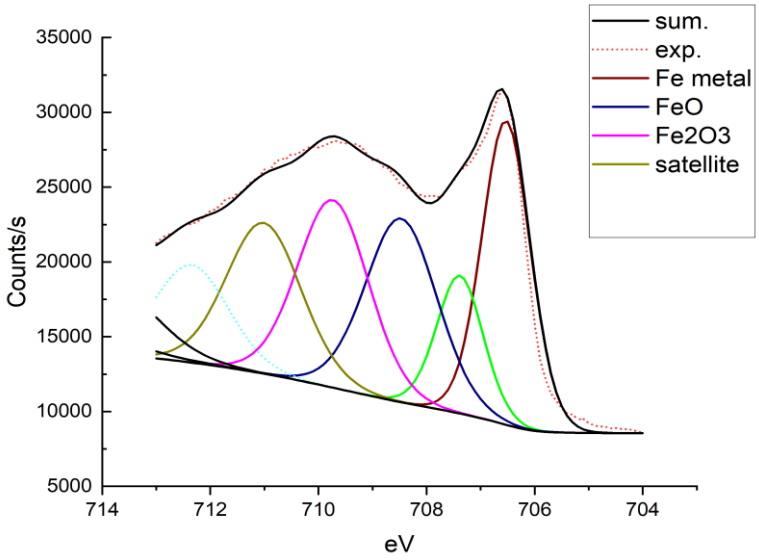

Fig. 9. Fitted XPS spectrum for iron corresponding to femtosecond laser treated surface marking

In the case of the femtosecond laser there can be found an amount of reduced iron with a peak at $706.53eV$ in Fig 14. with an atomic percentage of 14.21%. A small peak has been fitted at $707.37eV$ to make the curve fit the measured one more accurately. Different from the nanosecond treated surface the amount of spinel had reduced as an individual peak was not found in the analysis though the peak of the satellite from the reduced metal overlaps the spot on the spectrum where the spinel compound was found in the nanosecond surfaces, therefore the spike from spinel would be consumed in the spike of the satellite. The chromium scan can be seen in Fig 15. The compound showed a spike at the $Cr\ metal$ at $573.99eV$ and the $Cr(III)oxide$ at $575.76eV$. Here as well as the iron scan the reduced chromium satellite overlaps the spot where the spinel compound was. The oxide peak was reduced compared to the nanosecond treated surface, in the nanosecond case two distinguishable sharp peaks formed the 3/2 spin component peak but here the peaks form a more singular combined peak. In the manganese scan, a larger structure overlapping the scan was estimated as seen in Fig 16. Different oxides were found from $640eV$ to $644eV$, no spike big enough was found for the spinel compound on the manganese spectrum. The reduced manganese metal compound from $638.60eV$. Nickel scan (Fig 11.) on the femtosecond laser differed the most from the nanosecond spectra. There can be found a bigger spike of nickel metal at $852.76eV$ and some amount of nickel oxide, though the area and the height of the oxide peak is relatively small. Same oxide peak at $855eV$ can be

found on the nanosecond samples but has been left out due to the relatively small atomic percentage compared to all the others.[7 8 9 11 12]

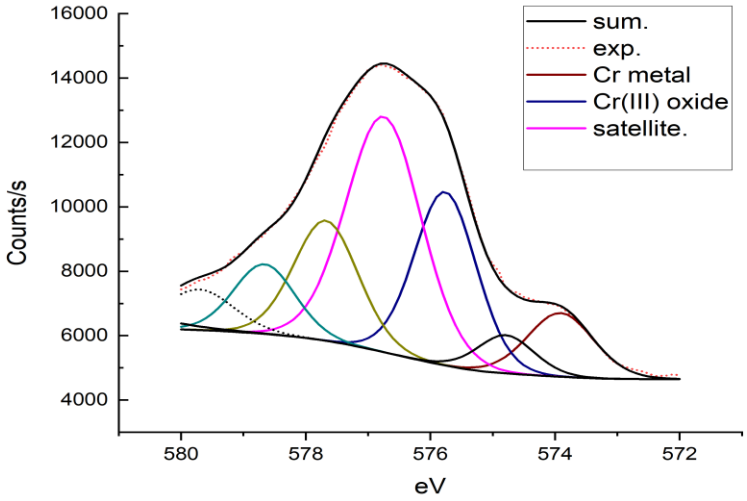

Fig. 10. Fitted XPS spectrum for chromium corresponding to femtosecond laser treated surface marking

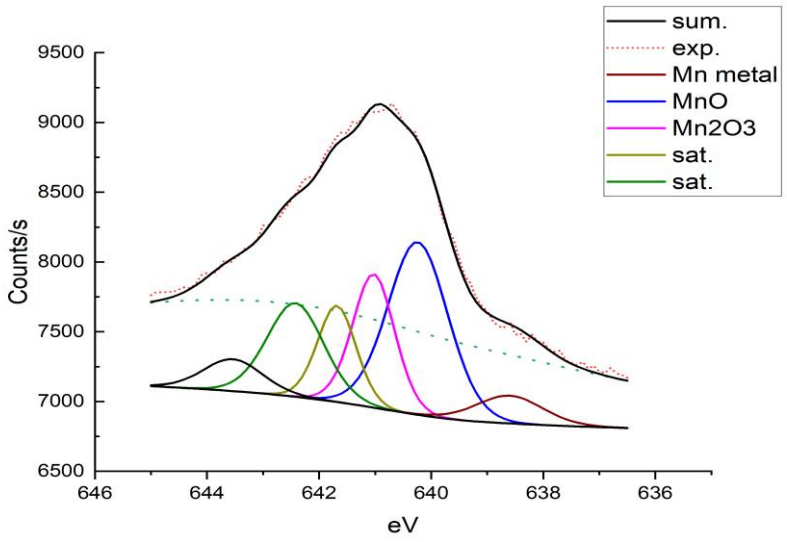

Fig. 11. Fitted XPS spectrum for manganese corresponding to femtosecond laser treated surface marking.

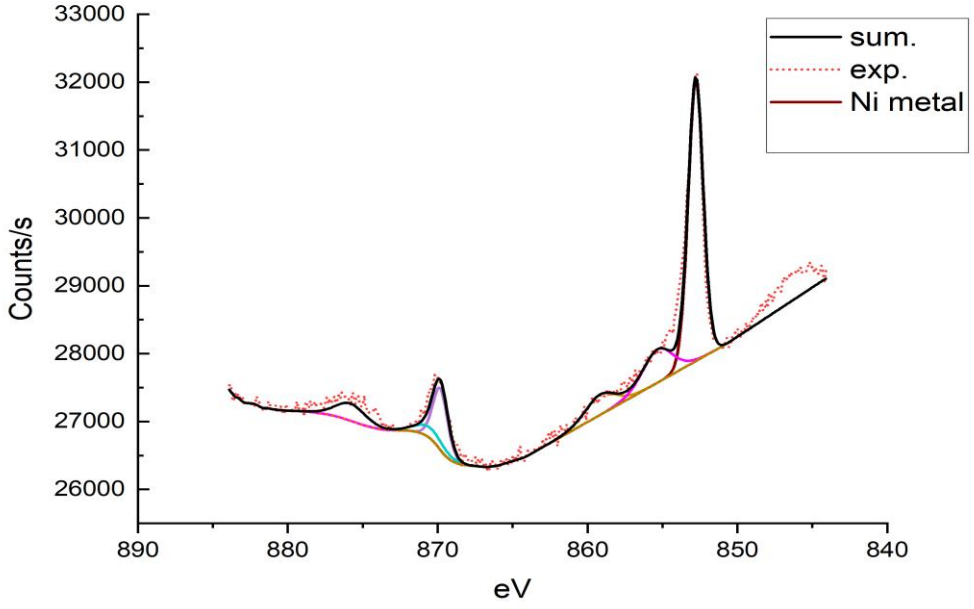

Fig. 12. Fitted XPS spectrum for nickel corresponding to femtosecond laser treated surface marking

4 Discussion

Table. 6. Laser treated surface characteristics.

Traits	Nanosecond Yellow	Nanosecond Blue	Nanosecond Red	Femtosecond
Visible grooves	No	No	No	Yes
Colour observed	-Oxide intrinsic -Non angle dependent	-Oxide intrinsic -Non angle dependent	-Oxide intrinsic -Non angle dependent	-Light diffraction -Angle dependent

In the SEM images the surfaces of the yellow and blue color seen similar in structure where on the surface can be seen randomly oriented wrinkles, whereas the red surface differs a bit where the difference comes from the small variations in components. The red surface SEM picture is also in a slightly different scale than the images of the yellow and blue surfaces which may affect the image. The femtosecond laser treated surface differs the most from the three others as there are clear grooves visible in a light interference sensitive scale. The random orientated wrinkles are in a much larger scale than visible light which suggests that the colour of the surface must come from the intrinsic colour of the surface compounds, and as the XPS fittings show, spinel compound was formed on the surface during the laser treatment .The nanosecond samples show a lot of similarity on what elements were found on the surface, therefore the differences in colour must come from different amounts of different elements. Spinel seems to be the dominating element taking into consideration the atomic percentages, though the oxides are ought to have their own contribution to the final colour that comes out after the treatment, and different oxides for example Fe^{3+} and Fe^{2+} have their own different hues of colour.

On the Fig.4 (d) can be seen the femtosecond laser treated surface SEM image. Here can be seen clear grooves made by the laser, which are in much smaller scale than in the other images. In conclusion the coloration on femtosecond markings on steel surface comes mainly from light interference with the surface. The XPS analysis shows how some of the metal has not produced spinel and oxides in such amounts due to the laser treatment as there was reduced metal found from the surface, along with this, the sum of the elements produces the base color of the treated

surface to metallic grey. Though in the angles where the light diffracts, can be observed a rainbow-like color. The diffractive surface can be found in nature for example on *morpho* butterflies seen in Fig.16, where the blue color comes primarily from the diffraction with the surface. The structure in micro- and nanoscale in the wing there can be seen a scale-like structure where the scales have oriented in different directions to reflect the light to all angles instead of only one like in the laser induced case. Each scale is then composed of a fine "Christmas-tree" structure that is ought to be the source for the coloration as the scale fits the wavelength of light.[13]

Fig. 13. Morpho menelaus butterfly with structural wing color.[14]

4.1 Conclusion

The anatomy of x-ray photoelectron spectroscopy was covered with a peak taken into the physics of atom physics and the origin of x-radiation and photoemission. The analysis of XPS spectra and different sources of peaks, e.g. Auger peaks were discussed. The study part of the thesis was about color produced on stainless steel 304 surface with a nanosecond- and femtosecond laser, then XPS measurements were taken and analyzed with Thermo Scientific Avantage software. The spectra of different elements were shown with the fittings and charts with the areas and atomic percentages. The origin of the color was figured to come from the intrinsic color of different metal oxides and spinel structures on the nanosecond case, instead with the femtosecond laser the dominating origin of the color was the color from light interfering with the nanostructure. The origin of the oxides and spinel is associated with the laser treatment. The future interests in the subject would be the possibilities of the structural coloration, as the structures could be modified so the color could be observed from all directions and the spectrum of colors seen could be directed from the whole spectrum at once to particular colors.

References

[1] https://en.wikipedia.org/wiki/X-ray_photoelectron_spectroscopy#History

[2] Pavlinsky GV. *Fundamentals of X-ray physics.* Cambridge: Cambridge International Science Publishing; 2008.

[3] Lu Y, Shi X, Huang Z, et al. Nanosecond laser coloration on stainless steel surface. *Scientific reports*. 2017;7(1):7092-8. doi: 10.1038/s41598-017-07373-8.

[4] H. Liu, W. Lin, M. Hong, 'Surface coloring by laser irradiation of solid substrates' *APL Photonics*, 4, 051101 (2019): doi: 10.1063/1.5089778.

[5] Wagner JM. *X-ray photoelectron spectroscopy.* New York: Nova Science Publishers, Inc; 2011. y

[6] http://www.xpsfitting.com/2012/08/spin-orbit-splitting.html

[7] Yamashita T, Hayes P. Analysis of XPS spectra of Fe2+ and Fe3+ ions in oxide materials. *Applied Surface Science*. 2008;254(8):2441-2449. doi: 10.1016/j.apsusc.2007.09.063.

[8] https://xpssimplified.com/

[9] W. Nesbitt H, BANERJEE D. Interpretation of XPS mn(2p) spectra of mn oxyhydroxides and constraints on the mechanism of MnO2 precipitation. *American Mineralogist*. 1997;83. doi: 10.2138/am-1998-3-414.

[10] Lu Y, Shi X, Huang Z, et al. Nanosecond laser coloration on stainless steel surface. *Scientific reports*. 2017;7(1):7092-8. doi: 10.1038/s41598-017-07373-8.

[11] Huang Z, Cai C, Wang G, Zhang H, Huttula M, Cao W. Structural color model based on surface morphology of MORPHO butterfly wing scale. *Surface Review and Letters*. 2016;23:1650046-1045. doi: 10.1142/S0218625X16500463

[12] Shi X, Huang Z, Laakso MJ, et al. Quantitative assessment of structural and compositional colors induced by femtosecond laser: A case study on 301LN stainless steel surface. *Applied Surface Science*. 2019;484:655-662. . doi: 10.1016/j.apsusc.2019.04.147

[13] Vorobyev AY, Guo C. Direct femtosecond laser surface nano/microstructuring and its applications. *Laser & Photonics Reviews*. 2013;7(3):385-407. doi: 10.1002/lpor.201200017.

[14] Huang Z, Cai C. Structural color model based on surface morphology of *Morpho* butterfly wing scale. *Surface Review and Letters*. 2016;Vol-23, No.5 1650046 https://doi.org/10.1142/S0328625X16500463